Available online at http://jprm.sms.edu.pk/
Journal of Prime Research in Mathematics, 21(1) (2025), 55–70

Journal of Prime Research in Mathematics

A Non-Integer Order Blood Rheological Model in a Magneto-thermal Environment

Azhar Ali Zafar[a,*], Maria Batool[a], Muhammad Shahzaib[a]

[a] *Department of Mathematics, Government College University, Lahore Pakistan.*

Abstract

This study develops a rheological model for blood flow in an arterial segment using a non-integer order derivative modelling in the sense of Atangana-Baleanu fractional derivative operator. This model takes into consideration the effects of external magnetic flux, periodic body acceleration, and radiant heat on the behaviour of the blood. Integral transforms are employed to solve the problem. Expressions for temperature, concentration, and flow velocity of blood will be developed. Additionally, the effects of the fractional order parameter and other important factors on blood dynamics are examined by the aid of analytical and graphical analysis and key findings are concluded that helps to control blood rheology.

Keywords: Coincidence point, MHD,, Integral transforms,, Blood flow,, Fractional order derivative operator.
2010 MSC: 76A05, 76A10.

1. Overview

The fractional calculus (FC) was discovered by the end of 17th century, as a result of the communication between Leibnitz and L'Hospital. Undoubtedly, FC is the broader version of classical calculus. FO derivative operators encapsulate the memory and heredity effects of many materials. By the end of 20th century, large amount of engineering literature, including various disciplines in mathematical biology, visco-elasticity, physics, and electrochemistry, carried out researrch by using the techniques of FC. For example, we refer the noteworthy contributions [1]-[6] and the references therein.
The comprehensive study of bio-fluids flow, subject to magnetic particles, paves the way for the new discipline known as bio-magnetic-fluid-dynamics (BMFD). Investigation into the new emerging BMFD is an interesting subject of research in the rheology of fluid. Bio-magnetic fluids exist in nature, that are present in living animals, influenced by magnetic field. Recently, due to its remarkable uses and applications in

*Corresponding author
Email addresses: azharalizafar@gcu.edu.pk (Azhar Ali Zafar), shamaria257@gmail.com (Maria Batool), m.shahzaib@gcu.edu.pk (Muhammad Shahzaib)

Received : 29 December 2024*; Accepted:* 01 May 2025*; Published Online:* 02 May 2025.

bioengineering and clinical sciences, for example, diminishing draining during medical procedures, magnetic gadget advancement for cell detachment, and the designated transport of medications, the BMFD has got much attention of the analysts.

Blood, being a bio-magnetic fluid, its flow pattern is significantly influenced by any snag in blood vessel. Moreover, the obstructed movement and action of blood vessels cause them to contract, known as, stenosis of blood vessels. The development of abnormalities in blood arteries, results in arteriosclerosis or stenosis. Blood consists of various types of cells suspended in plasma, which behaves as an incompressible Newtonian fluid. Blood has a density $1060kgm^{-3}$ and viscosity $3 \times 10^{-3}Pa$. Blood acts like a non-Newtonian fluid at low shear rates, particularly when it passes across narrow veins, yet plasma flows like a Newtonian fluid in thin streams. Furthermore, the oxygenation level of blood impacts its magnetic characteristics [7]. Blood circulation can be disturbed by external accelerations, such as those experienced when flying in aeroplanes, riding in rockets, dealing with punching or drilling tools, and participating in sports like high jumping and surfing. An elevated pulse rate, headaches, vision loss, and, in certain situations, cardiovascular problems can result from prolonged exposure to such conditions.

Motivated by the bio-magnetic nature of blood, many successful attempts have been made to model and control the blood rheology. For instance, see [8, 9, 10, 11, 12, 13], for the case in which blood is considered as Newtonian fluid. Furthermore, blood as non-Newtonian fluid and being an electrically conducting fluid is considered in [14]-[20]. When blood flows through an artery with a diameter greater than 0.025 cm, it behaves like a Newtonian fluid [21], [22]. However, blood is considered a Casson fluid when it flows through smaller arteries under low shear conditions [23]. Various flow models describing blood rheology have been developed using FC techniques. For instance, Saqib et al. [24] numerically solved a mathematical model involving magnetohydrodynamic (MHD) blood flow in the presence of dusty particles, utilizing a non-integer order approach. In [25] Delgado et al. applied a FO method to examine oxygen tissue-level diffusion through the blood stream. He et al. [26] also used FC to study blood flow through capillaries, incorporating multiple forces into their model. Additionally, Shah et al. conducted further investigations into non-integer order models in blood flow research [27]. The rheological behaviour of blood with magnetically responsive particles and periodic motion stimuli was examined by Riaz and Zafar [28]. The two-phase flow of blood through arteries is investigated in [29]. In [30], Awrejcewicz et al. by treating blood as a Newtonian fluid investigated the blood rheology in the femoral and coronary arteries under the influence of oscillating pressure gradients, external magnetic fields, and periodic body acceleration. Furthermore, Maiti et al. [31] addressed the influence of thermal and mass flux on the blood rheology by presenting a non-integer order model for magnetohydrodynamic (MHD) fluid flow using the Caputo Fabrizio fractional derivative operator. In 2016, Atangana and Baleanu [32] presented a new derivative operator called Atangana-Baleanu-derivative-operator in the sense of Caputo (ABC). The intricate character of many physical phenomena may be displayed by this operator that lacks in regular as well as in many FO operators. Compared to Caputo and Caputo-Fabrizio derivative operators, ABC is more generic yet has regular smooth kernel. Moreover, ABC is proven to be more suitable for dynamical models influenced by heat effects.

Following the previous discussion, we will explored and examined blood rheology using uniformly suspended magnetic particles while being affected by radiant heat, oscillating pressure gradients, and periodic body acceleration. A Casson fluid, which is a shear-thinning non-Newtonian fluid with high viscosity at low shear rates, will be utilised to represent blood. The investigation of blood flow behaviour in a porous medium will be taken into account by utilizing the impacts of radiant heat and external body acceleration. Additionally, a non-dimensional corresponding mathematical model will be constructed using the ABC fractional derivative operator. Integral transforms will be used to solve the model, and the expressions for temperature, concentration, and flow velocity will be obtained. Additionally, graphical analysis will be used to examine how the FO parameter and other significant influence of the parameters on the blood rheology.

Our research design is as follows; After introduction, we have nomenclature, where representation of symbols with bar are dimensional quantities while without bar are non dimensional quantities. In section 2, we give the description of the mathematical framework of the problem. In section 3, we formulate the FO model, in section 4, we have elaborated the solution procedure. While, section 5 is dedicated to graphical analysis

and finally notable findings are documented in section 6.

Nomenclature

Symbol	Description	Symbol	Description
U_f	Axial velocity of blood	D_m	Mass diffusibility
T_f	Temperature of blood	K_T	Ratio of thermal diffusion
C_f	Concentration of blood	T_∞	Ambient temperature
ρ	Blood density	U_o	Average velocity of blood
K_p	Permeability constant	R	Constant radius of artery
β	Casson number	T_w	Wall temperature
σ	Electric conductivity	C_w	Concentration of wall
B_o	Intensity of magnetic field	C_∞	Ambient concentration
g	Acceleration due to gravity	D_a	Darcy number
β_T	Thermal expansion coefficient	G_r	Thermal Grashof number
β_C	Concentration coefficient	G_m	Solutal Grashof number
$G(T)$	Body acceleration	H_a	Hartman number
A_o	Amplitude of body acceleration	S_c	Schmidt number
k	Frequency of body acceleration	Re	Reynold number
ϕ	Phase angle	Pr	Prandtl number
K	Thermal conductivity	Sr	Soret number
C_p	Specific heat capacity	R	Radiation parameter
Q_m	Metabolic heat source	Pe	Peclet number
θ_m	Heat absorption	b_o	Invariable amplitude of pressure
β_1	Heat absorption coefficient		gradient
Ω	Frequency	b_1	Pulsatile amplitude component
B	Plank's constant	ω	Pulsatile frequency

2. Mathematical Framework for the Problem

Assume that blood passes through an artery segment with an internal radius R_o and length L like a Casson fluid. Moreover, blood rheology is established using radiant heat, periodic body acceleration, and an external magnetic field. During blood flow, these factors significantly change the rheological properties of blood.The flow is assumed to be unidirectional as it moves through a micro-channel, where the induced magnetic field is much weaker than the external magnetic field. The momentum equation is formulated, like in [33]-[34] as;

$$\frac{\partial \bar{U}_f}{\partial \bar{t}} = -\frac{1}{\rho}\frac{\partial \bar{P}}{\partial \bar{z}} + \upsilon\left(1+\frac{1}{\beta}\right)\left[\frac{\partial^2 \bar{U}_f}{\partial \bar{r}^2} + \frac{1}{\bar{r}}\frac{\partial \bar{U}_f}{\partial \bar{r}}\right] + G(\bar{t}) - \frac{\upsilon}{k_p}\bar{U}_f - \sigma\frac{B_o^2 \bar{U}_f}{\rho} + g\beta_H(\bar{T}_f - T_\infty) + g\beta_c(\bar{C}_f - C_\infty). \quad (2.1)$$

As seen in [35], [36], and [37], the body acceleration can be expressed as;

$$G(\bar{t}) = \bar{A}_o cos(\bar{k}\bar{t} + \phi). \tag{2.2}$$

As used in [34], [38], the energy equation derived under the influence of thermal radiation is evolved as (cf. [34])

$$\frac{\partial \bar{T}_f}{\partial \bar{t}} = \frac{\mathcal{K}}{c_p \rho}\left[\frac{\partial^2 \bar{T}_f}{\partial \bar{r}^2} + \frac{1}{\bar{r}}\frac{\partial \bar{T}_f}{\partial \bar{r}}\right] - \frac{1}{c_p \rho}\frac{\partial \bar{q}}{\partial \bar{r}} + \frac{\bar{\theta} m + \bar{Q} m}{c_p \rho}. \tag{2.3}$$

Under the assumption of low heat absorption coefficient and density for blood, heat flux is approximated as (cf. [34])

$$-\frac{\partial \bar{q}_r}{\partial \bar{r}} = (2\beta_1)^2(\bar{T}_f - T_\infty). \tag{2.4}$$

According to [39], the concentration equation for the Soret effect which occurs when moving particles with varying molecular sizes combine can be expressed by;

$$\frac{\partial \bar{C}_f}{\partial \bar{t}} = D_m\left[\frac{\partial^2 \bar{C}_f}{\partial \bar{r}^2} + \frac{1}{\bar{r}}\frac{\partial \bar{C}_f}{\partial \bar{r}}\right] + \frac{K_T D_m}{T_\infty}\left[\frac{\partial^2 \bar{T}_f}{\partial \bar{r}^2} + \frac{1}{\bar{r}}\frac{\partial \bar{T}_f}{\partial \bar{r}}\right]. \tag{2.5}$$

The initial and boundary conditions (IBCs) listed below are taken into consideration.

$$\begin{aligned} &\bar{C}_f = 0,\ \bar{T}_f = 0,\ \bar{U}_f = 0, \quad for\ 0 \le \bar{r} \le R_0,\ at\ \bar{t} = 0, \\ &\frac{\partial \bar{T}_f}{\partial \bar{r}} = 0,\ \frac{\partial \bar{C}_f}{\partial \bar{r}} = 0,\ \frac{\partial \bar{U}_f}{\partial \bar{r}} = 0, \quad at\ \ \bar{r} = 0, \\ &\bar{T}_f = T_\omega,\ \bar{U}_f = 0,\ \bar{C}_f = C_\omega, \quad for\ \bar{r} = R_0\ \ and\ \bar{t} > 0. \end{aligned} \tag{2.6}$$

The following dimensional descriptors are introduced as:

$$\begin{aligned} &\zeta = \frac{\bar{r}}{R_0},\ U_f = \frac{\bar{U}_f}{U_0},\ P = \frac{\bar{P}}{\rho U_0^2},\ T_f = \frac{\bar{T}_f - T_\infty}{T_\omega - T_\infty},\ z = \frac{\bar{z}}{R_0},\ k = \frac{\bar{k} R_0}{U_0},\ \tau = \frac{U_0 \bar{t}}{R_0}, \\ &\theta m = \frac{R_0 \bar{\theta m}}{U_0 \rho c_p (T_\omega - T_\infty)}, C_f = \frac{\bar{C}_f - C_\omega}{C_\omega - C_\infty},\ A_0 = \frac{R_0 \bar{A}_0}{U_0^2},\ Qm = \frac{R_0 \bar{Q m}}{u_0 \rho c_p (T_\omega - T_\infty)}. \end{aligned} \tag{2.7}$$

After the non-dimensionalization, the equations (2.1), (2.3), and (2.5) transformed into

$$\begin{aligned} \frac{\partial U_f}{\partial \tau} =& -\frac{\partial P}{\partial z} + \frac{1}{Re}\left(1 + \frac{1}{\beta}\right)\left[\frac{\partial^2 U_f}{\partial \zeta^2} + \frac{1}{\zeta}\frac{\partial U_f}{\partial \zeta}\right] + A_0 cos(kt + \phi) - \frac{1}{DaRe}F - \frac{Ha^2}{Re}U_f \\ &+ \frac{Gr}{Re^2}T_f + \frac{Gm}{Re^2}C_f, \end{aligned} \tag{2.8}$$

$$Pe\frac{\partial T_f}{\partial \tau} = \left[\frac{\partial^2 T_f}{\partial \zeta^2} + \frac{1}{\zeta}\frac{\partial T_f}{\partial \zeta}\right] + RT_f + Pe(\theta m + Qm), \tag{2.9}$$

$$ReSc\frac{\partial C_f}{\partial \tau} = \left[\frac{\partial^2 C_f}{\partial \zeta^2} + \frac{1}{\zeta}\frac{\partial C_f}{\partial \zeta}\right] + SrSc\left[\frac{\partial^2 T_f}{\partial \zeta^2} + \frac{1}{\zeta}\frac{\partial T_f}{\partial \zeta}\right], \tag{2.10}$$

where

$$\begin{aligned} &Gr = \frac{\beta_T g(T_f\omega - T_f\infty)R_0^3}{\upsilon^2},\ Da = \frac{k_p}{R_0^2},\ Ha^2 = \frac{\sigma(B_0 R_0)^2}{\rho\upsilon},\ Gm = \frac{\beta_C g(C_f\omega - C_f\infty)R_0^3}{\upsilon^2} \\ &Sc = \frac{\upsilon}{Dm},\ Pr = \frac{c_p \mu}{K},\ Re = \frac{U_0 R_0}{\upsilon},\ Sr = \frac{k_T Dm(T_f\omega - T_f\infty)}{\upsilon T_f\infty(C_f\omega - C_f\infty)},\ R = \frac{4\alpha_1^2 R_0^2}{k},\ Pe = PrRe. \end{aligned} \tag{2.11}$$

The analogous initial and boundary conditions are

$$\begin{aligned} &U_f(\zeta,0)=0,\ T_f(\zeta,0)=0,\ C_f(\zeta,0)=0, && at\ \tau=0,\ \zeta\in[0,1]\\ &\frac{\partial U_f}{\partial\zeta}=0,\ \frac{\partial T_f}{\partial\tau}=0,\ \frac{\partial C_f}{\partial\tau}=0, && at\ \zeta=0,\\ &U_f(1,\tau)=0,\ T_f(1,\tau)=0,\ C_f(1,\tau)=0, && at\ \tau>0. \end{aligned} \tag{2.12}$$

For cardiovascular function the expression for pressure gradient is represented as;

$$-\frac{\partial P}{\partial z}=b_0+b_1\cos(\omega\tau). \tag{2.13}$$

3. Fractional Analogue of the Problem

The fractional analogue of the model is obtained by replacing the time derivative operator by D_t^α in the sense of ABC

$$\begin{aligned} D_\tau^\alpha U_f(\zeta,\tau)=&b_0+b_1\cos(\omega\tau)+\frac{1}{Re}\Big(1+\frac{1}{\beta}\Big)\left[\frac{\partial^2U_f}{\partial\zeta^2}+\frac{1}{\zeta}\frac{\partial U_f}{\partial\zeta}\right]+A_0cos(k\tau+\phi)-\frac{1}{ReDa}U_f-\frac{Ha^2}{Re}U_f\\ &+\frac{Gr}{Re^2}T_f+\frac{Gm}{Re^2}C_f, \end{aligned} \tag{3.1}$$

$$Pe\ D_\tau^\alpha T_f=\left(\frac{\partial^2T_f}{\partial\zeta^2}+\frac{1}{\zeta}\frac{\partial T_f}{\partial\zeta}\right)+RT_f+Pe(\theta m+Qm), \tag{3.2}$$

$$ScRe\ D_\tau^\alpha C_f=\left(\frac{\partial^2C_f}{\partial\zeta^2}+\frac{1}{\zeta}\frac{\partial C_f}{\partial\zeta}\right)+SrSc\left(\frac{\partial^2T_f}{\partial\zeta^2}+\frac{1}{\zeta}\frac{\partial T_f}{\partial\zeta}\right). \tag{3.3}$$

Here, D_t^α is ABC FO derivative operator like in [32] defined as,

$$D_\tau^p(f(\tau))=\frac{M(p)}{1-p}\int_0^\tau f'(x)E_p[-p\frac{(\tau-x)^p}{1-p}]dx, \tag{3.4}$$

In this context p $(0<p<1)$ represents the non integer order parameter and $M(p)$ is the normalization function, which can be any function that satisfies $M(0)=M(1)=1$. For instance, it could be $M(p)=1+\frac{p}{\Gamma(p+1)}-p$. For the purposes of this study, we have chosen $M(p)=1$. Additionally, E_p refers to the well known Mittag-Leffler function [40].
Furthermore, Laplace transform of the ABC is;

$$L\{D_\tau^pf(\tau)\}=\frac{M(p)q^pLf(\tau)}{(1-p)q^p+p}-\frac{M(p)q^{p-1}f(0)}{(1-p)q^p+p}.$$

4. Computational Framework

The mathematical model will be solved by using integral transforms. Employing Laplace transform on equation (3.1)-(3.3) by using IC (12), yields

$$\begin{aligned} \left(\frac{x_1q^\alpha+y_1}{x_2q^\alpha+y_2}\right)U_f(\zeta,q)=&\frac{b_0}{q}+b_1\frac{q}{q^2+\omega^2}+\frac{1}{Re}\left(1+\frac{1}{\beta}\right)\left[\frac{\partial^2U_f(\zeta,q)}{\partial\zeta^2}+\frac{1}{\zeta}\frac{\partial U_f(\zeta,q)}{\partial\zeta}\right]\\ &+A_0\left(\frac{q\cos\phi-k\sin\phi}{q^2+k^2}\right)+\frac{G_r}{Re^2}T_f(\zeta,q)+\frac{G_m}{Re^2}C_f(\zeta,q), \end{aligned} \tag{4.1}$$

$$\left(\frac{(Pe-R(1-\alpha))q^{\alpha}-R\alpha}{(1-\alpha)q^{\alpha}+\alpha}\right)T_f(\zeta,q)=\left[\frac{\partial^2 T_f}{\partial\zeta^2}+\frac{1}{\zeta}\frac{\partial T_f}{\partial\zeta}\right]+Pe(\theta m+Qm), \tag{4.2}$$

$$ScRe\,\frac{q^{\alpha}}{(1-\alpha)q^{\alpha}+\alpha}C_f(\zeta,q)=\left[\frac{\partial^2 C_f}{\partial\zeta^2}+\frac{1}{\zeta}\frac{\partial C_f}{\partial\zeta}\right]+SrSc\left[\frac{\partial^2 T_f}{\partial\zeta^2}+\frac{1}{\zeta}\frac{\partial T_f}{\partial\zeta}\right], \tag{4.3}$$

here $x_1=DaRe+(1-\alpha)(1+DaHa^2),\ x_2=DaRe(1-\alpha),\ y_1=(1+DaHa^2)\alpha,\ y_2=DaRe\alpha.$
Employing the Hankel transform to equation (4.1)-(4.3), yield

$$\begin{aligned}U_f(\zeta_n,q)=&\left(\frac{x_2q^{\alpha}+y_2}{x_3q^{\alpha}+y_3}\right)\left(\left[\frac{b_0}{q}+b_1\frac{q}{q^2+\omega^2}+A_0\left(\frac{q\cos\phi-k\sin\phi}{q^2+k^2}\right)\right]\frac{J_1(\zeta_n)}{\zeta_n}\right.\\&\left.+\frac{G_r}{Re^2}T_f(\zeta_n,q)+\frac{G_m}{Re^2}C_f(\zeta_n,q)\right),\end{aligned} \tag{4.4}$$

$$T_f(\zeta_n,q)=\frac{\delta.Pe(\theta m+Qm)}{y_4q}\left(\frac{q^{\alpha}+\gamma}{q^{\alpha}+\gamma_1}\right)\frac{J_1(\zeta_n)}{\zeta_n}, \tag{4.5}$$

$$C_f(\zeta_n,q)=y_5\left(\frac{(q^{\alpha}+\gamma)(q^{\alpha}+\gamma)}{q(q^{\alpha}+x_4)(q^{\alpha}+\gamma_1)}\right)J_1(\zeta_n), \tag{4.6}$$

where $U_f(\zeta_n,q)=\int_0^1 rU_f(\zeta,q)J_2(\zeta\zeta_n)d\zeta\ =$ is the finite Hankel transform of the function $U_f(\zeta,q)$ and $\zeta_n; n=1,2...$ are positive roots of transcendental equation $J_2(x)=0$, J_ν being Bessel function of first kind of order ν. Moreover, into above relations $x_3=x_1+(\frac{1}{Re}(1+\frac{1}{\beta})\zeta_n^2)x_2,\ y_3=y_1+(\frac{1}{Re}(1+\frac{1}{\beta})\zeta_n^2)y_2, \delta=(1-\alpha), y_4=PrRe+(-R+\zeta_n^2)\delta,$
$y_5=-\frac{\zeta_n SrScPe(Qm+\theta m)\delta}{(ReSc+\zeta_n^2(1-\alpha))y_4},\ \gamma=\frac{\alpha}{(1-\alpha)},\ x_4=\frac{\zeta_n^2\alpha}{(ReSc+\zeta_n^2\delta)}$ and $\gamma_1=\frac{(-R+\zeta_n^2)\alpha}{y_4}$.

Next, using the relations (A1)-(A3) from the Appendix and applying inverse LT on (4.4)-(4.6), we obtain

$$\begin{aligned}U_f(\zeta_n,\tau)=&\frac{x_2}{x_3}\frac{J_1(\zeta_n)}{\zeta_n}\big(b_0a_1(\tau)+b_1a_2(\tau)+A_0(a_3(\tau)-a_4(\tau))+\ \psi_1[a_5(\tau)+q_1a_6(\tau)+q_2a_7(\tau)]+\\&\psi_2[a_8(\tau)+q_5a_9(\tau)+q_6a_{10}(\tau)+q_7a_{11}(\tau)]\big).\end{aligned} \tag{4.7}$$

$$T_f(\zeta_n,\tau)=\frac{J_1(\zeta_n)}{\zeta_n}\Big[a_{12}(\tau)+a_{13}(\tau)\Big], \tag{4.8}$$

$$C_f(\zeta_n,\tau)=\ \psi_3\Big[a_{14}(\tau)+q_3a_{15}(\tau)+q_4a_{16}(\tau)\Big]J_1(\zeta_n). \tag{4.9}$$

where
$a_1(\tau)=[E_{\alpha,1}(\psi_5\tau^{\alpha})+\psi_4\tau^{\alpha}E_{\alpha,1+\alpha}(\psi_5\tau^{\alpha})],$
$a_2(\tau)=[\tau^{2k}E_{\alpha,1+2k}(-y_2\tau^{\alpha})+\psi_4\tau^{\alpha+2k}E_{\alpha,\alpha+1+2k}(-\psi_5\tau^{\alpha})],$
$a_3(\tau)=\cos\phi\sum_{l=0}^{\infty}(-1)^l[(\tau^{2n}E_{\alpha,2l+1}(\psi_5\tau^{\alpha})+\psi_4\tau^{\alpha+2l}E_{\alpha,\alpha+2l+1}(\psi_5\tau^{\alpha})],$
$a_4(\tau)=\sin\phi\sum_{l=0}^{\infty}(-1)^l[\big(\tau^{2l+1}E_{\alpha,2l+2}(\psi_5\tau^{\alpha})+\psi_4\tau^{\alpha+2l+1}E_{\alpha,\alpha+2l+2}(\psi_5\tau^{\alpha})\big),$

$$a_5(\tau)=\sum_{l=0}^{\infty}\sum_{m=0}^{\infty}\frac{(-q_2)^i(-q_1)^j\binom{l+m}{m}}{\Gamma(m(2\alpha-\alpha+2(l+1)\alpha-2\alpha+1)}\tau^{(m+2l)\alpha},$$
$$a_6(\tau)=\sum_{l=0}^{\infty}\sum_{m=0}^{\infty}\frac{(-q_2)^l(-q_1)^m\binom{l+m}{j}}{\Gamma(m(2\alpha-\alpha+2(l+1)\alpha-2\alpha+1)}\tau^{(m+2l+1)\alpha},$$
$$a_7(\tau)=\sum_{l=0}^{\infty}\sum_{m=0}^{\infty}\frac{(-q_2)^l(-q_1)^m\binom{l+m}{m}}{\Gamma(m(2\alpha-\alpha+2(l+1)\alpha-2\alpha+1)}\tau^{(m+2l+2)\alpha},$$

$$a_8(\tau)=\sum_{l=0}^{\infty}\sum_{m=0}^{\infty}\sum_{n=0}^{\infty}\tbinom{l+m+n+1}{l}\tbinom{l+m}{m}(-1)^{l+m+n}(q_8)^n(q_9)^m(q_{10})^l\quad\left[\frac{\tau^{3\alpha l+2\alpha m+\alpha n-1}}{3\alpha l+2\alpha m+\alpha n}\right],$$
$$a_9(\tau)=\sum_{l=0}^{\infty}\sum_{m=0}^{\infty}\sum_{n=0}^{\infty}\tbinom{l+m+n+1}{n}\tbinom{l+m}{m}(-1)^{l+m+n}(q_8)^n(q_9)^m(q_{10})^l\quad\left[\frac{\tau^{3\alpha l+2\alpha m+\alpha n+\alpha}}{\Gamma(3\alpha l+2\alpha m+\alpha n+\alpha+1}\right],$$
$$a_{10}(\tau)=\sum_{l=0}^{\infty}\sum_{m=0}^{\infty}\sum_{n=0}^{\infty}\tbinom{l+m+n+1}{l}\tbinom{l+m}{m}(-1)^{l+m+n}(q_8)^n(q_9)^m(q_{10})^l\quad\left[\frac{\tau^{3\alpha l+2\alpha m+\alpha n+2\alpha}}{\Gamma(3\alpha l+2\alpha m+\alpha n+2\alpha+1}\right],$$
$$a_{11}(\tau)=\sum_{l=0}^{\infty}\sum_{m=0}^{\infty}\sum_{n=0}^{\infty}\tbinom{l+m+n+1}{l}\tbinom{l+m}{m}(-1)^{l+m+n}(q_8)^n(q_9)^m(q_{10})^l\quad\left[\frac{\tau^{3\alpha l+2\alpha m+\alpha n+3\alpha}}{\Gamma(3\alpha l+2\alpha m+\alpha n+3\alpha+1}\right].$$

$$a_{12}(\tau)=\psi_1E_{\alpha,1}(\gamma\tau^{\alpha}),$$
$$a_{13}(\tau)=\psi_1\gamma_1E_{\alpha,1+\alpha}(\gamma_1\tau^{\alpha}),$$

$$a_{14}(\tau)=\sum_{l=0}^{\infty}\sum_{m=0}^{\infty}\frac{(-q_2)^l(-q_1)^m\binom{l+m}{m}}{\Gamma\big((m+2l)\alpha+1\big)}\tau^{(m+2l)\alpha},$$
$$a_{15}(\tau)=\sum_{l=0}^{\infty}\sum_{m=0}^{\infty}\frac{(-q_2)^l(-q_1)^m\binom{l+m}{m}}{\Gamma\big((m+2l+1)\alpha+1\big)}\tau^{(m+2l+1)\alpha},$$
$$a_{16}(\tau)=\sum_{l=0}^{\infty}\sum_{m=0}^{\infty}\frac{(-q_2)^l(-q_1)^m\binom{l+m}{m}}{\Gamma\big((m+2l+2)\alpha+1\big)}\tau^{(m+2l+2)\alpha}.$$

and $\psi_1=\frac{G_r}{Re^2}\frac{Y_4.PrRe(Qm+\theta m)}{y\delta}$, $\psi_2=y_5r_n\frac{G_m}{Re^2}$, $\psi_3=\frac{y_4.PrRe(Qm+\theta m)}{\delta s}$, $\psi_4=\frac{y_2}{x_2}$, $\psi_5=\frac{y_3}{x_3}$, $q_1=\psi_4+\gamma$, $q_2=\psi_4\gamma$,
$q_3=\psi_5+\gamma_1$, $q_4=\psi_5\gamma_1$, $q_5=2\gamma+\psi_4, q_6=\gamma(\gamma+\psi_4)+\psi_4\gamma$, $q_7=\gamma^2\psi_4$,
$q_8=x_4+\gamma_1+\psi_5q_6$, $q_9=\gamma_1(x_4+\psi_5)+x_4\psi_5$, $p_{10}=x_4\gamma_1\psi_5$.
Employing Inverse Hankel Transform to equations (4.7)-(4.9) generates

$$\begin{aligned}U_f(\zeta,\tau)=&2\frac{x_2}{x_3}\sum_{n=1}^{\infty}\frac{J_0(\zeta\zeta_n)}{J1(\zeta_n)}\frac{1}{(\zeta_n)^2}\Big(a_1(\tau)+a_2(\tau)+a_3(\tau)-a_4(\tau)\\&+\psi_1[a_5(\tau)+q_1a_6(\tau)+q_2a_7(\tau)]+\psi_2[a_8(\tau)+q_5a_9(\tau)+q_6a_{10}(\tau)+q_7a_{11}(\tau)]\Big),\end{aligned}\tag{4.10}$$

$$T_f(\zeta,\tau)=2\sum_{n=1}^{\infty}\frac{J_0(\zeta\zeta_n)}{J1(\zeta_n)}\frac{1}{(\zeta_n)^2}\Big[a_{12}(\tau)+a_{13}(\tau)\Big],\tag{4.11}$$

$$C_f(\zeta,\tau)=2\sum_{n=1}^{\infty}\frac{J_0(\zeta\zeta_n)}{J1(\zeta_n)}\frac{1}{\zeta_n}\psi_3\Big[a_{14}(t)+q_3a_{15}(\tau)+q_4a_{16}(\tau)\Big].\tag{4.12}$$

It is important to highlight that our results can be used to derive several findings from the existing literature. For example, in the context of $\frac{1}{\beta} = 0$, $\beta_T = 0$ and $\beta_c = 0$, our model provides the results of Awrejcewicz et al. [30]. Additionally, by setting $G(t) = 0$ (thereby neglecting the effects of body acceleration), our model further produces the results obtained by Zafar et al. [29]. As α approaches unity, the model behavior corresponds. Furthermore, by choosing $\beta_T = 0$ and $\beta_c = 0$ we recover the results presented in [23]. Lastly, our model is consistent with the one presented by Bansi et al. [34] when $\frac{1}{\beta} = 0$ and $\beta_c = 0$ are assumed.Furthermore, the authors of [34] used the Caputo derivative operator to apply a fractional order model and describe blood as a Newtonian fluid. But according to [32], the Atangana-Baleanu derivative operator is more suited for models with thermal effects. Consequently, our model offers a more dependable foundation in terms of mathematical formulation and fluid dynamics.

5. Graphs and Discussion

In this section, we will explore various factors influencing the velocity and temperature of blood subjected to magnetic flux and external body acceleration, utilizing graphical analysis with MATHCAD 15.We will specifically look at the effects of non-dimensional characteristics on blood temperature and velocity, including the Darcy number, Casson number, radiation number, fractional order parameters, and Hartmann number.

The following parametric values will be fixed for numerical simulations: $A_o = 0.6$, $\beta = 0.3$, $b_o = 0.002$, $b_1 = 0.005$, $\omega = \frac{\pi}{7}$, $\phi = 0.1$ $\kappa = \frac{\pi}{4}$,and $Da = 0.00012$,. Furthermore, the parameters that have been used provide varying values so that we may examine how they influence the rheology of the blood.

The fractional parameter α is essential for regulating blood velocity. Figure 1 shows the velocity plotted against time for a range of α values. The findings show that blood velocity increases in tandem with an increase in α.

As illustrated in Fig. 2, the Thermal Grashof number is used to analyse and debate heat transfer by free convection. It has been seen that when the Thermal Grashof number rises, so does the velocity. This is because free convection from the heat gradient and temperature variations affects the fluid's velocity. Generally speaking, temperature and density have a reciprocal connection, which raises fluid velocity.

The Solutal Grashof number, which is the ratio of the species buoyancy force to the viscous hydrodynamic force, is another variation of the Grashof number that is shown in Fig. 3. One can see that the Solutal Grashof number trend is nearly the reverse of the thermal Grashof number trend, with a higher Solutal Grashof number resulting in a lower flow velocity.

It is clear from Fig. 4 that velocity profiles ascend with increasing Peclet number, whereas velocity plots decrease with decreasing Peclet number. This indicates a direct proportionality between the velocity and the Peclet number. The Peclet number behaves in the opposite direction from the Reynolds number in a large variety of mass and energy transfer situations. We can learn more about the properties of the flow surrounding the boundary layers by examining this parameter. In addition, it should be mentioned that the performance of the thermal boundary layer is either enhanced or decreased in relation to the flow behaviour of the momentum boundary layer by the product of the Prandtl number and Reynolds number. Fig. 5 shows a similar trend for the Peclet number when compared to Qm. The figure illustrates how blood velocity rises as the metabolic heat source value rises and falls when the metabolic heat source value falls. But as Qm increases, the axial velocity remains increasing. Another important element affecting the temperature distribution of blood flow is the parameter θm. The body's temperature is controlled by this heat absorption characteristic. As can be shown in Fig. 6, the velocity profile increases as the value of θm increases.

The shear component of momentum diffusivity divided by the mass transfer diffusivity is known as the Schmidt number. It is employed to describe fluid flow in which mass diffusion involves both convection and instantaneous momentum mechanisms. In essence, it demonstrates the connection between the boundary layers in mass transfer and the thickness of the hydrodynamic layers. An opposite trend is seen when

looking at how the Schmidt number affects the velocity profile, as seen in Fig. 7. This suggests that when the Schmidt number rises, the velocity profile falls, and vice versa. This behaviour results from the Schmidt number's impact on density and heat-mass transport mechanisms.
Figure 8 illustrates the impact of the Soret number on blood velocity. The ratio between the temperature differential and the fluid's concentration is represented by the Soret number. The gradient is steeper and the temperature differential is larger when the Soret number is higher. As a result, varying Soret number values cause the fluid velocity to decrease because of the higher thermal diffusion factor.
Figures 9-12 show the profiles of temperature for various material parameters. for instance, the temperature profile changes as the radiation parameter R varies, as seen in Figure 9. It is clear that when thermal radiation rises, the temperature rises as well. Additionally, Figure 10 depicts how α affects the temperature profiles. It is evident that changing α has an important effect on the temperature distribution, with the increasing values of alpha within the unit interval, temperature also increases.
As Peclet number offers important information about the properties of the boundary layer flow and controls the transfer of thermal energy. With the increasing values of Peclet number Figure 11 shows that the temperature profiles grow as well. A crucial factor in the transfer of thermal energy is the Peclet number, which is comparable to the Reynolds number. Another important component that has a major impact on the bloodstream's temperature distribution is the metabolic heat source (Qm). The interior temperature of the body is regulated in part by this heat source. Heat production in the body is regulated by metabolic activities, specifically the quantity of mitochondria per cell. Therefore, as Figure 12 illustrates, the metabolic heat source (Qm) is closely correlated with the rise in blood temperature that occurs.

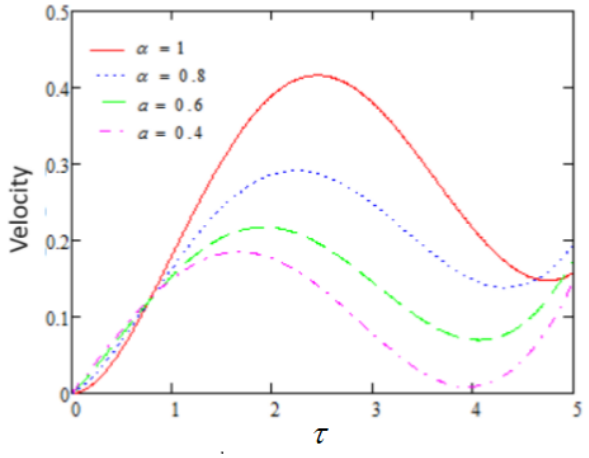

Figure 1: Profiles of U_f versus τ for different values of α

6. Final Remarks

This paper presents a fractional order mathematical model using the ABTFDO to describe the flow of incompressible non-Newtonian blood through blood vessels, considering the effects of periodic body acceleration, an external magnetic field, and radiant heat. The Laplace transform and the zero-order finite Hankel transform are used to solve the non-dimensional velocity, temperature, and concentration of suspended magnetic particles in the blood cells. Furthermore, the effects of temperature, metabolic heat source, radiation parameter, and fractional order parameter on blood flow are examined graphically. Key observations from the study are outlined below:

- Velocity of the blood flow depends independently on the non-integer order parameter α, as the value of α increases, velocity also increases.

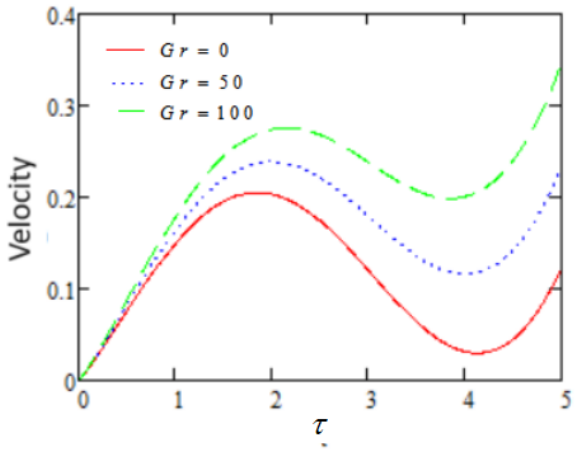

Figure 2: Profiles of U_f versus τ for different values of Gr

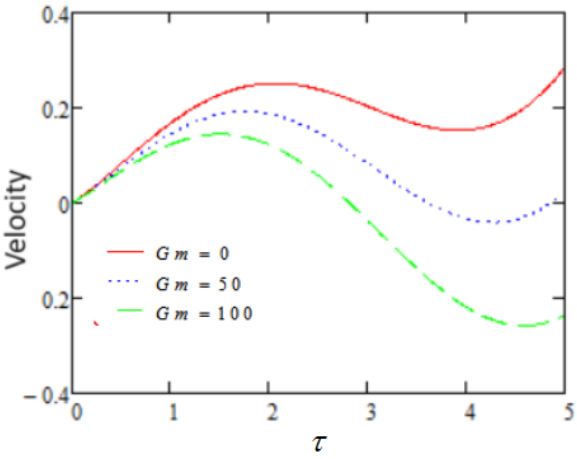

Figure 3: Profiles of U_f versus τ for different values of Gm

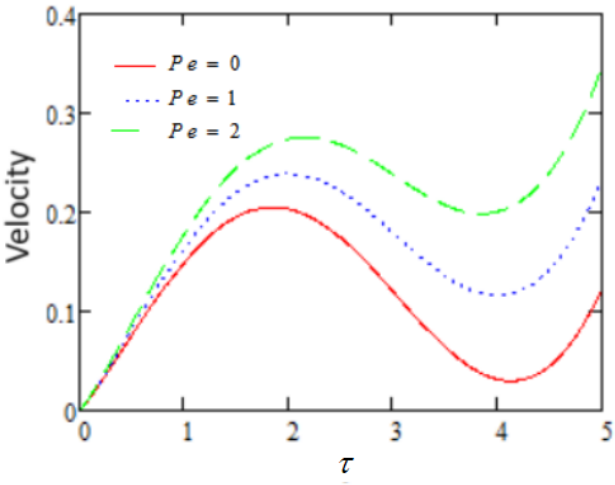

Figure 4: Profiles of U_f versus τ for different values of Pe

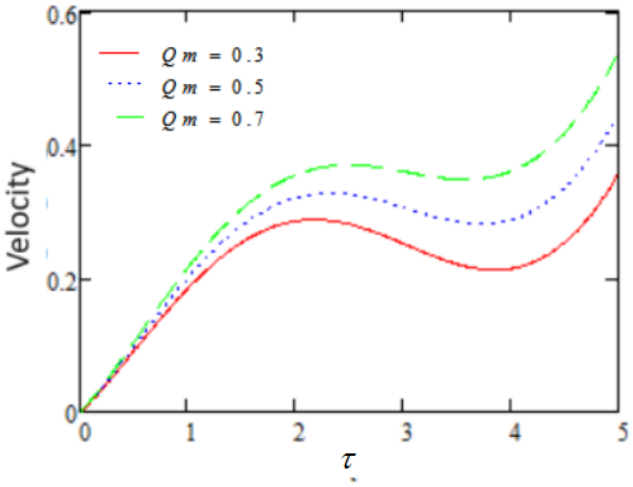

Figure 5: Profiles of U_f versus τ for different values of Qm

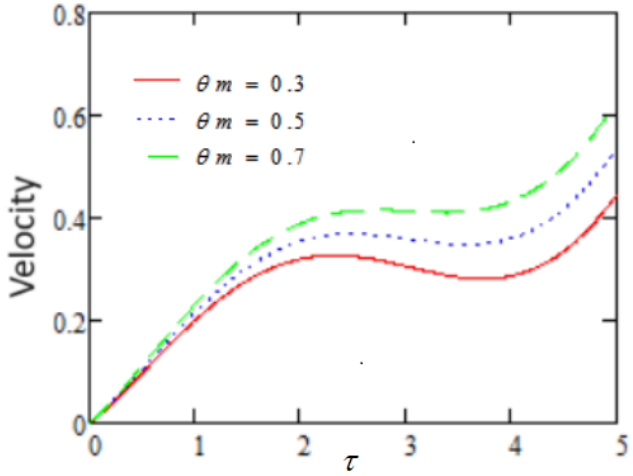

Figure 6: Profiles of U_f versus τ for different values of θm

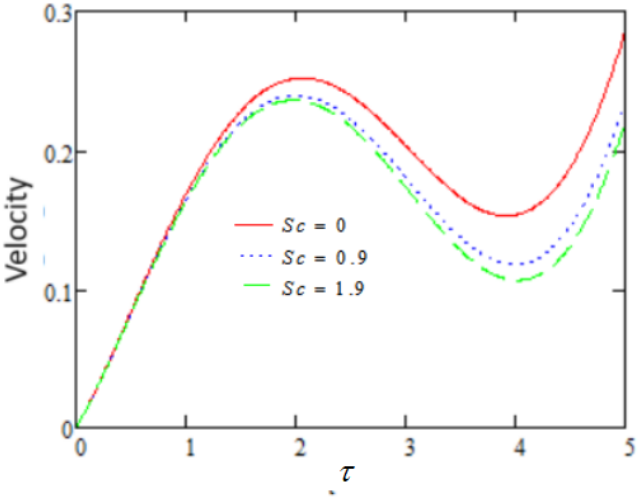

Figure 7: Profiles of U_f versus τ for different values of Sc

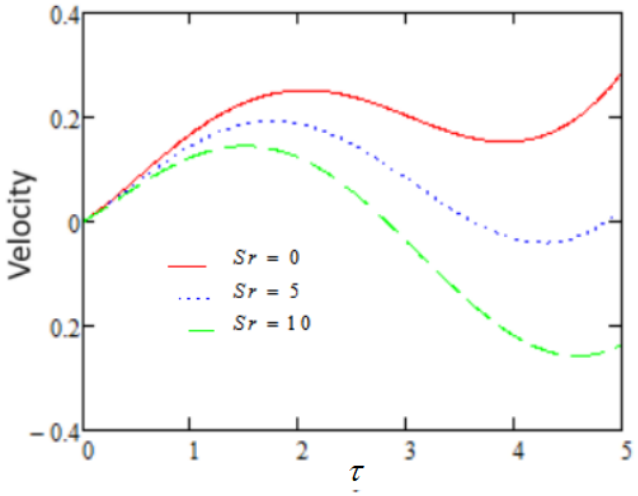

Figure 8: Profiles of U_f versus τ for different values of Sr

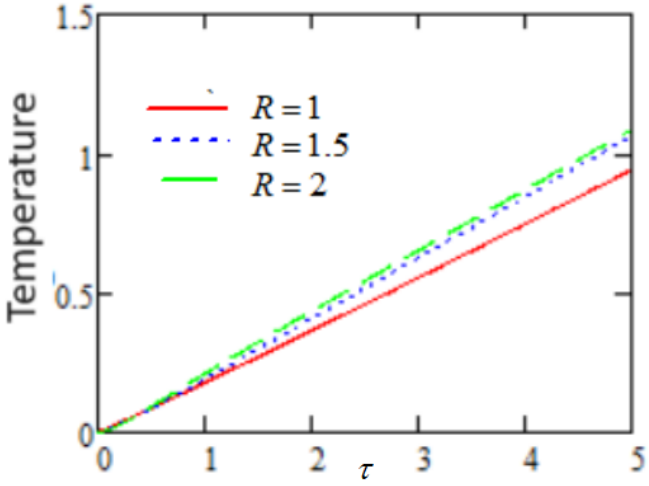

Figure 9: Profiles of T_f versus τ for different values of R

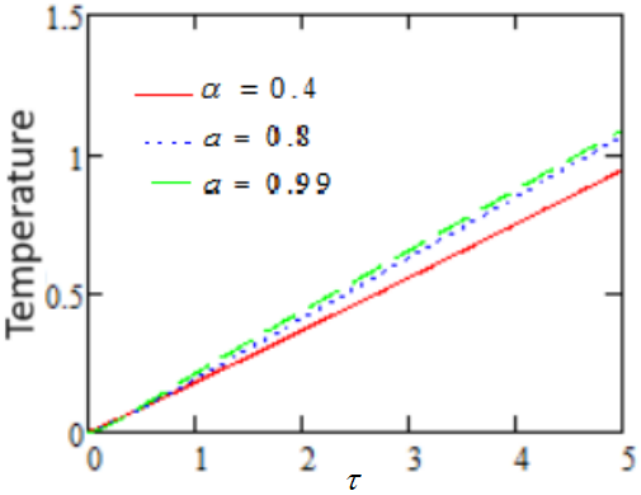

Figure 10: Profiles of T_f versus τ for different values of α

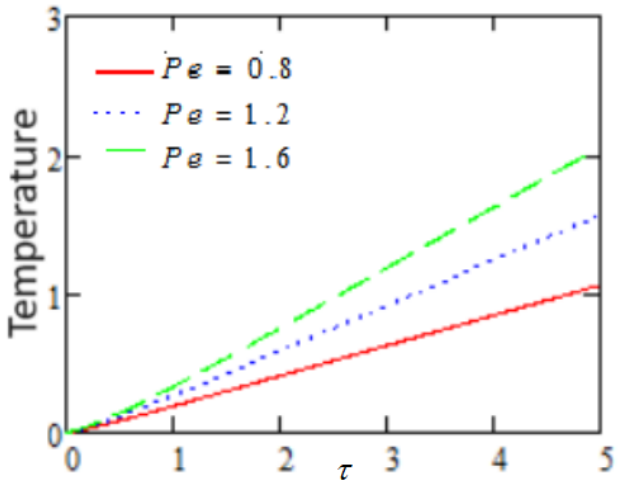

Figure 11: Profiles of T_f versus τ for different values of Pe

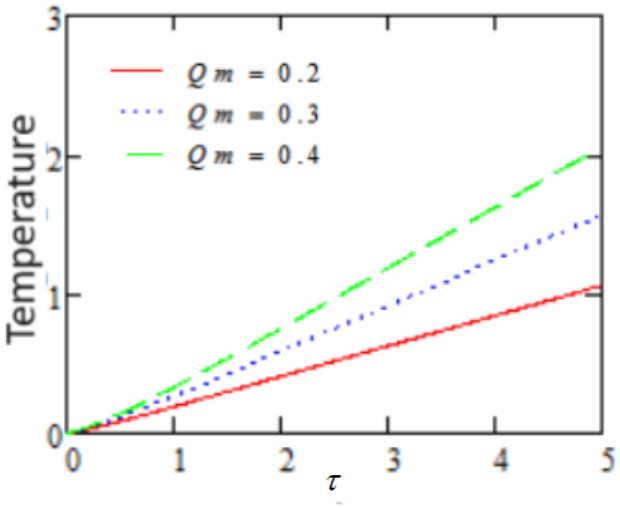

Figure 12: Profiles of T_f versus τ for different values of Qm

- Also an increase in the thermal Grashof number, makes the velocity of the blood to increase, on the other hand an increase in Solutal Grashof number, makes the velocity to decrease.
- Also observations show that the velocity of the blood increases as the value of the metabolic heat source, heat absorption and radiation parameter increases, while, it decreases with the increase of Schmidt number and Soret number.
- Temperature of the blood is directly proportional to the radiation parameter, non-integer order parameter, metabolic heat source and Peclet number.

APPENDIX

$$\mathcal{L}^{-1}\{\frac{q^{a-b}}{q^a-\alpha}\} = \tau^{b-1}E_{a,b}(\alpha\tau^a). \tag{A1}$$

$$\mathcal{L}^{-1}\left\{\frac{q^c}{\alpha q^a+\beta q^b}\right\} = \tau^{a-c-1}\sum_{l=0}^{\infty}\sum_{m=0}^{\infty}\frac{(-\beta)^l(-\alpha)^m\binom{l+m}{m}}{\Gamma\big(m(a-b)+(l+1)a-c\big)}\tau^{m(a-b)+la}. \tag{A2}$$

$$\begin{aligned}\mathcal{L}^{-1}\left\{\frac{q^a}{q^b+\alpha q^c+\beta q^d+\gamma}\right\} &= \sum_{l=0}^{\infty}\sum_{m=0}^{\infty}\sum_{n=0}^{\infty}\binom{l+m+n}{n}\\ &\binom{l+n}{m}(-1)^{l+m+n}(\alpha)^n(\beta)^m(\gamma)^l\Big[\frac{\tau^{b(l+m+n+1)-a-dm-cn-1}}{\Gamma(b(l+m+n+1)-a-dm-cn)}\Big].\end{aligned} \tag{A3}$$

Acknowledgements

The authors would like to thank anonymous reviewers for their careful assessment and useful suggestions that helped us to improve the manuscript. Moreover, we are highly thankful and grateful to the Office of Research Innovation and Commercialization (ORIC), Government College University, Lahore, Pakistan, for generous support and facilitating this research work.

Funding

This work is the part of the ORIC funded faculty research project No. 422/ORIC/24 "Theoretical study of the rheology of biological fluids in human body in the presence of magnetic particles using fractional calculus modeling approach."

Conflicts of Interest

The authors declare no conflict of interest.

References

[1] S. G. Samko, A. A. Kilbas, O. I. Marichev, Fractional integrals and derivatives: Theory and Applications, Gordon and Breach Science Publishers, 1993. 1

[2] S. Das, Functional fractional calculus for system identification and controls, Springer, 2008.

[3] K. Oldham, J. Spanier, The Fractional Calculus, Academic Press, 1974.

[4] M .D. Ortigueira, Fractional Calculus for Scientists and Engineers, Springer, New York, 2011.

[5] D. Baleanu, K. Diethelem, E. Scales, J. J. Trujillo, Fractional calculus models and numerical methods, World Scientific Publishing Company, Singapore, 2012.

[6] S. Sharma, U. Singh, V. K. Katiyar, Magnetic field effect on flow parameters of blood along with magnetic particles in a cylindrical tube. J. Magn. Magn. Mater; 377:395401, 2015.doi: 10.1016/j.jmmm.2014.10.136 1

[7] A. K. Maiti, Mathematical modelling on blood flow under atherosclerotic condition, American Journal of Applied Mathematics, 4(6), 324- 329, 2016. doi: 10.11648/j.ajam.20160406.19 1

[8] E. W. Merrill ,A. M. Benis, E. R. Gilliland, T. K. Sherwood,E. W. Salzman, Pressure flow relations of human blood in hollow fibers at low flow rates. J. Appl Physiol; 20(50): 95467,1965.doi: 10.1152/jappl.1965.20.5.954 1

[9] J. C. Chow Blood flow: theory, effective viscosity and effects of particle distribution. Bull Math Biol; 37:47188, 1975. doi: 10.1007/BF02459515 1

[10] J. Wang, Y. Huang, A. E. David et al., Magnetic nanoparticles for MRI of brain tumors, Current Pharmaceutical Biotechnology, 13(12), 24032416, 2012. doi: 10.2174/138920112803341824 1

[11] S. C. McBain, H. H. Yiu, and J. Dobson, Magnetic nanoparticles for gene and drug delivery, International Journal of Nanomedicine, 3(2), 16980, 2008. doi: 10.2147/ijn.s1608 1

[12] G. C. Shit, S. Majee, Pulsatile flow of blood and heat transfer with variable viscosity under magnetic and vibration environment, J. Magn. Magn. Mater. 388 106-115, 2015. doi: 10.1016/j.jmmm.2015.04.026 1

[13] J. C. Misra, G. C. Shit, Flow of a biomagnatic visco-elastic fluid in a channel with streching walls, J. Appl. Mech. 76(6), 061006, 2009. doi: 10.1115/1.3130448 1

[14] A. Mondal, G. C. Shit, Transport of magneto-nanoparticles druging electro-smotic flow in a micro-tube in the presence of magnetic field for drug delivary application, J. Magn. Magn. Mater. 442, 319-328, 2017. doi: 10.1016/j.jmmm.2017.06.131 1

[15] M. M. Bhatti, A. Zeeshan, R. Ellahi, Simultaneous effects of coagulation and variable magnetic field on peristaltically induced motion of Jeffrey nanofluid containing gyrotactic microorganism, Microvasc. 110, 32-42, 2017. doi: 10.1016/j.mvr.2016.11.007

[16] M. Abdulhameed, D. Vieru, R. Roslan, Modeling electro-magnetohydrodynamic thermo-fluidic transport of biofluids with new trend of fractional derivative without singular kernel, Physica A, 484, 233- 252, 2017. doi: 10.1016/j.physa.2017.05.001

[17] M. M. Bhatti, A. Zeeshan, R. Ellahi, Endoscope analysis on peristaltic blood flow of Sisko-fluid with titanium magneto-nanoparticles, Comput. Biol. Med. 78, 29-41, 2016. doi: 10.1016/j.compbiomed.2016.09.007

[18] A. Zeeshan, M. M. Bhatti, N. S. Akbar, Y. Sajjad, Hydromagnetic blood flow of Sisko fluid in a non-uniform channel induced by Peristaltic wave, Commun. Theor. Phys. 68, 103-110, 2017. doi: 10.1088/0253-6102/68/1/103

[19] S. Majee, G. C. Shit, Numerical investigation of MHD flow of blood and heat transfer in a stenosed arterial segment, J. Magn. Magn. Mater. 424, 137-147, 2017. doi: 10.1016/j.jmmm.2016.10.028

[20] N. S. Akbar, A. W. Butt, Entropy generation analysis in convective ferromagnetic nano blood flow through a composite stenosed arteries with permeable wall, Commun. Theor. Phys. 67, 554-560, 2017. doi:10.1088/0253-6102/67/5/554 1

[21] D. A. McDonald, On steady flow through modeled vascular stenosis, Journal Pre-proof 12(1), 13-20, 1979. doi: 10.1016/0021-9290(79)90004-6 1

[22] C. G. Caro, T. J. Pedley, R. C. Schroter, W. A. Seed, The Mechanics of the Circulation, Cambridge University Press, 2012. 1

[23] F. Ali, N. A. Sheikh, I. Khan, M. Saqib, Magnetic field effect on blood flow of Casson fluid in axisymmetric cylindrical tube: A fractional model, J. Magn. Magn. Mater. 423, 327-336, 2017. doi: 10.1016/j.jmmm.2016.09.125 1, 4

[24] M. Saqib, I. Khan, S. Shafie, Generalized magnetic blood flow in a cylindrical tube with magnetite dusty particles, J. Magn. Magn. Mater. 484, 490-496, 2019. doi: 10.1016/j.jmmm.2019.03.032 1

[25] V. F. Morales-Delgado, J. F. Gmez-Aguilar, K. M. Saad, M. A. Khan, P. Agarwal, Analytic solution for oxygen diffusion from capillary to tissues involving external force effects: A fractional calculus approach, Physica A, 523, 48-65, 2019. doi: 10.1016/j.physa.2019.02.018 1

[26] S. He, N. A. A. Fataf, S. Banerjee, K. Sun, Complexity in the muscular blood vessel model with variable fractional derivative and external disturbances, Physica A, 526, 120-904, 2019. doi: 10.1016/j.physa.2019.04.140 1

[27] N. A. Shah, D. Vieru, C. Feteacu Effects of the fractional order and magnetic field on the blood flow in cylindrical domains. J. Magn. Magn. Mater; 409:10-19, 2016. doi:10.1016/j.jmmm.2016.02.013 1

[28] M. B. Riaz, A. A. Zafar, Exact solutions for the blood flow through a circular tube under the influence of a magnetic field using fractional Caputo-Fabrizio derivatives, Math Model Nat Phenom; 13(8), 2018. doi: 10.1051/mmnp/2018005 1

[29] A. A. Zafar , N. A. Shah, I. Khan, Two phase flow of blood through a circular tube with magnetic properties. J Magn Magn Mater; 477:382-387, 2019. doi: 10.1016/j.jmmm.2018.08.035 1, 4

[30] J. Awrejcewicz, A. A. Zafar, G. Kudra, M. B. Riaz, Theoretical study of the blood flow in arteries in the presence of magnetic

particles and under periodic body acceleration, Chaos Solitons and Fractals, 140, 2020. doi:10.1016/j.chaos.2020.110204 1, 4

[31] S. Maiti, S. Shaw, G. C. Shit, CaputoFabrizio fractional order model on MHD blood flow with heat and mass transfer through a porous vessel in the presence of thermal radiation, Physica A: Statistical Mechanics and its Applications, 540, 123-149, 2020. doi: 10.1016/j.physa.2019.123149 1

[32] A. Atangana and D. Baleanu, New fractional derivatives with non-local and non-singular kernel: theory and applications to heat transfer method, Thermal Sci. 20, 763-769, 2016. doi: 10.2298/TSCI160111018A 1, 3, 4

[33] F. Ali, N. A. Sheikh, I. Khan, M. Saqib, Magnetic field effect on blood flow of Casson fluid in axisymmetricc cylindrical tube: A fractional model, J. Magn. Magn. Mater. 423, 327-336, 2017. doi: 10.1016/j.jmmm.2016.09.125 2

[34] C. D. K. Bansi, C. B. Tabi, T. G. Motsumi, A. Mohamadoud, Fractional blood flow in oscillatory arteries with thermal radiation and magnetic field effects, J. Magn. Magn. Mater. 456, 38-45, 2018. doi: 10.1016/j.jmmm.2018.01.079 2, 2, 2, 4

[35] V. K. Sud, G. S. Sekhon, Blood flow subject to a single cycle of body acceleration, Bull. Math. Biol, 46, 937-949, 1984. doi: 10.1016/S0092-8240(84)80012-9 2

[36] P. Chaturani, V. Palanisamy, Casson fluid model for pulsatile flow of blood under periodic body acceleration, Biorheology, 27(5); 619-630, 1990. doi: 10.3233/BIR-1990-27501 2

[37] G. C. Shit, M. Roy, Pulsatile flow and heat transfer of a magnetomicropolar fluid through a stenosed artery under the influence of body acceleration, J. Mech. Med. Biol. 11(3); 643-661,2011. doi: 10.1142/S0219519411003909 2

[38] T. Chinyoka, O. D. Makinde, Computational dynamics of arterial blood flow in the presence of magnetic field and thermal radiation therapy, Adv. Math. Phys. 915-640, 2014. doi: 10.1155/2014/915640 2

[39] T. Hayat, H. Zahir, A. Tanveer, A. Alsaedi, Influences of Hall current and chemical reaction in mixed convective peristaltic flow of Prandtl fluid, J. Magn. Magn. Mater. 407; 321-327, 2016. doi: 10.1016/j.jmmm.2016.02.020 2

[40] M. G. Mittag-Leffler. Sur la nouvelle fonction $E_\alpha(x)$. Proc. Paris Academy of Science, 554-558, 1903b. doi: 10.4236/apm.2013.31017 3

[41] A. Wiman, Ueber den Fundamentalsatz in der Theorie der Funkilionen $E_\alpha(x)$. Acta. Math. 29; 91201, 1905. doi: 10.12691/ajma-3-2-2.

[42] R. Gorenflo, A. A. Kilbas, F. Mainardi, S. V. Rogosin, Mittag-Leffler functions, related topics and applications, Springer, Berlin, 2016.

[43] S. Kazem, Exact solution of some linear fractional differential equations by Laplace transform, International Journal of nonlinear science 16(1): 3-11, 2013.

[44] S. S. Sajjadi ,D. Baleanu, A. Jajarmi, H. M.Pirouz, A new adaptive synchronization and hyperchaos control of biological snap oscillator, Chaos Soliton Fract 138: 109919; 2020. doi: 10.1016/j.chaos.2020.109919

[45] R. Gorenflo, A. A. Kilbas,F. Mainardi, S. V. Rogosin, Mittag-Leffler Functions. In Related Topics and Applications, Springer, Germany, 2014.